Curr Radiol Rep (2019) 7:26
https://doi.org/10.1007/s40134-019-0337-5

COMPUTED TOMOGRAPHY (S NICOLAOU AND M MOHAMMED, SECTION EDITORS)

Vascular Imaging: Utilization of Dual-Energy Computed Tomography

Ahmed Alharthy[1,3] · Matthew D'Mello[2] · Hatim Alabsi[1,3] · Nicolas Murray[1] · Omar Metwally[1] · Khaled Y. Elbanna[1] · Mohammed F. Mohammed[1,4] · Faisal Khosa[1]

Published online: 17 July 2019

Abstract
Purpose of Review The goal of this review is to present a concise summary of the current literature on the use of dual-energy computed tomography (DECT) for vascular imaging.
Recent Findings DECT techniques have shown significant promise and useful applications for the detection of subtle pulmonary embolism, intramural hematoma, active bleeding, and differentiation of bleed from contrast staining in the brain, with potentially less radiation and improved accuracy.
Summary Vascular imaging with DECT has many new applications through enhanced technology and postprocessing algorithms.

This article is part of the Topical collection on *Computed Tomography*.

✉ Faisal Khosa
fkhosa@hotmail.com

[1] Department of Radiology, Vancouver General Hospital, University of British Columbia, 899 12th Avenue West, Vancouver, BC V5Z 1M9, Canada

[2] Faculty of Medicine, University of British Columbia, 317-2194 Health Sciences Mall, Vancouver, BC V6T 1Z3, Canada

[3] Department of Radiology, Faculty of Medicine, King Abdulaziz University Hospital, King Abdulaziz University, Jeddah, Saudi Arabia

[4] Abdominal Imaging Section, Medical Imaging Department, King Saud bin Abdulaziz University for Health Sciences, King Abdullah International Medical Research Center, Ministry of the National Guard, Health Affairs, Riyadh, Saudi Arabia

Keywords Dual-energy computed tomography · Vascular imaging · Endoleak · Aortic imaging · Lower limb angiography · Vascular trauma imaging

Introduction

Dual-energy computed tomography (DECT) is an emerging technology in the field of medical imaging with a variety of vascular applications. As opposed to conventional computed tomography (CT) that emits x-rays from a single source at a single peak energy level (often 120 kVp) in which x-rays are received by a single detector set, DECT has the advantage of analyzing the interaction of materials submitted to two energy levels (often 80 and 140 kVp) to generate additional data.

Currently, three DECT systems have gained favor in the clinical setting (Table 1). This review will specifically focus on dual-source DECT as it is the primary form of DECT employed at our institution. The principles of DECT and its general application in vascular imaging will be reviewed followed by a discussion on specific vascular imaging applications.

Principles of DECT

Conventional CT relies on two phenomena: the photoelectric effect and Compton scattering [1]. In brief, the photoelectric effect is the attenuation observed when a photon expels an electron from the innermost orbit (k-shell) of an atom. The likelihood of expelling an electron increases with high atomic number materials (iodine and calcium) at low-range energies because the photon energy needed to exceed the k-shell of these materials (k-edge)

Table 1 Comparison of DECT systems

System type	Vendor	Description
Dual source	Siemens Healthcare	Two sources of energy located 90° to each other Two receivers simultaneously acquire data
Fast kV switching Single source	GE Healthcare	Single source producing alternately high and low energies Single receiver
Single-source dual-layer detector system	Philips Healthcare	Single source of energy Two-layer (sandwich) receiver detects two energy levels

closely matches the low-energy source. Elements with low atomic numbers (hydrogen, oxygen, and carbon) attenuate both low- and high-energy sources at a relatively equal rate due to both energy sources not matching their low k-edge values. Two different materials may display similar attenuation values when submitted to a given level of energy, such as iodine and calcium, depending on their relative concentration. Given that DECT uses information from two energy levels (high and low), body constituents made of different materials will have a distinct spectral signature. The low-energy beam in DECT enables the exploitation of the photoelectric effect for material characterization [2]. For an in-depth discussion on the principles of DECT, readers are referred to the White Paper on DECT series of articles [3–6].

General Application in Vascular Imaging

Three-Material Decomposition

A major component of DECT is the processing of unique spectral data. DECT postprocessing software can deconstruct each voxel based on the presence of three base materials (fat, iodine, and soft tissue) on a dual-source DECT system by comparing the attenuation of each material at high and low energies. Decomposition is carried out on the basis of attenuation coefficients [7]. DECT postprocessing techniques have numerous applications in acute care settings [8–14]. DECT is particularly useful for vascular imaging with respect to creating virtual unenhanced images [15] and bone removal [16].

Virtual unenhanced imaging can also be created following a contrast-enhanced study with DECT to mimic true unenhanced images. Since each voxel is decomposed into three materials, the resulting image can be constructed with or without iodine content simulating either an angiographic image or true unenhanced image, respectively [15]. Consequently, the unenhanced acquisition necessary for angiographic imaging may be eliminated altogether with DECT. This reduces radiation exposure to the patient and time in the scanner.

Bone-removal imaging is based on a similar concept in which each voxel is examined for calcium, iodine, and blood. The voxels that contain bone are targeted and assigned a low attenuation value (− 1024 Hounsfield units). Thus, bone is largely invisible to the viewer, and a clear image of the blood vessels is provided. This is particularly useful in imaging craniocervical and peripheral arterial vasculature [16]. Compared to conventional angiographic imaging, DECT allows for more accurate visualization of the vascular supply through tortuous bony structures in the body, especially those in which bone is intimately associated with vessels such as the intercostal arteries [17].

Virtual Monochromatic Images

Virtual monochromatic images (VMIs) are images created with DECT data that simulate images obtained from a true monochromatic (or monoenergetic) source. Conventional CT, despite its heavy filtration, is polychromatic with photon energies displaying a large range. DECT algorithms can process the two polychromatic beams in a DECT scanner to create VMIs. The key advantage of VMIs for vascular imaging is the ability to reduce the beam hardening observed with the absorption of low-energy photons coming from the polychromatic beam. VMIs created at low keV levels can more closely approximate the k-edge of contrast, thus increasing the attenuation of iodine, improving the contrast resolution between structures and allowing a reduction in the amount of contrast needed to obtain similar quality images [18]. The application of VMI at higher energy levels to vasculature surrounding stents, clips, and coils helps to reduce artifacts and improves visualization [19].

Head and Neck

Brain Hemorrhage

With respect to imaging of the head, DECT is most useful in differentiating new intermittent hemorrhage versus contrast staining after intra-arterial recanalization/revascularization (IAR). A well-known adverse outcome, new hemorrhage is reported to occur in up to 15% of patients receiving IAR [20]. Unfortunately, contrast staining of the parenchyma due to blood–brain barrier breakdown also occurs at approximately the same time post-IAR [21]. Differentiating the two phenomena is challenging because iodinated contrast and blood have very similar CT attenuation values (Fig. 1). DECT is ideal for identifying potentially catastrophic post-IAR bleed because DECT algorithms can separate blood, iodine, and soft tissue based on spectral signals. Specifically, the contribution of iodine to the image can be calculated (iodine mapping) and then subtracted from the blended image to create a VNC image. Use of both iodine mapping and VNC has been shown to increase the positive predictive value and overall accuracy in hemorrhage detection post-IAR [22••].

DECT is also advantageous over conventional CT angiography during the initial identification and characterization of active bleeding (Fig. 2). The spot sign is a radiographic sign that presents as a hyperdense area on contrast-enhanced imaging and is strongly associated with both active bleeding as well as postdetection mortality [23]. The use of iodine mapping and VNC images as previously described works well to identify hemorrhage with the added advantage of reduced radiation because no nonenhanced scan is required with DECT (compared to conventional CT angiography, which requires serial scans).

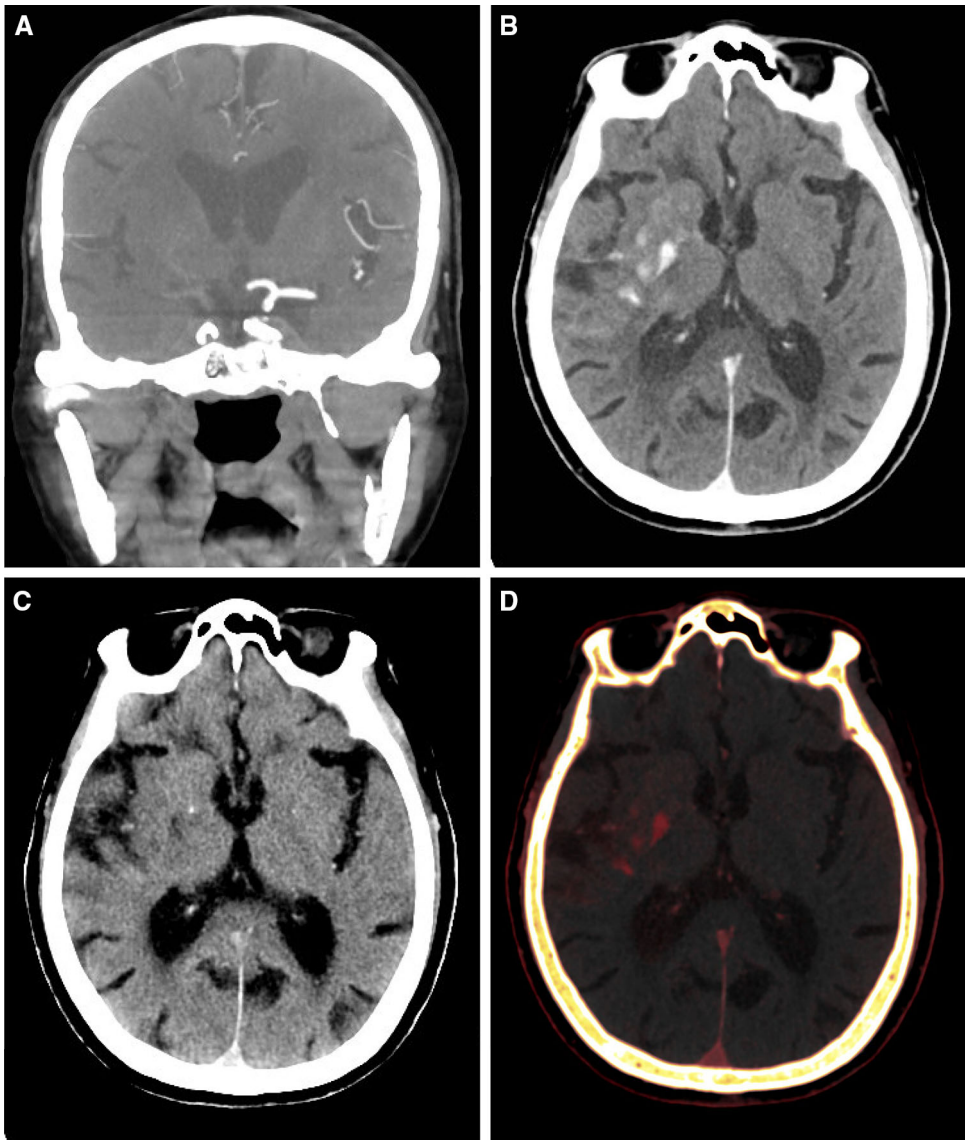

Fig. 1 Contrast staining **a** CTA demonstrated occlusion of the right ICA supraclinoid segment, right M1, and right A1 segments. Catheter angiography and endovascular thrombectomy were performed. **b** 3 h postintervention CT study demonstrated patchy areas of high attenuation in the right basal ganglia which could be contrast or acute blood. **c** VNC demonstrated Substraction of the basal ganglia high attenuation areas, in keeping with contrast staining (**d**) iodine overlay confirmed the contrast staining

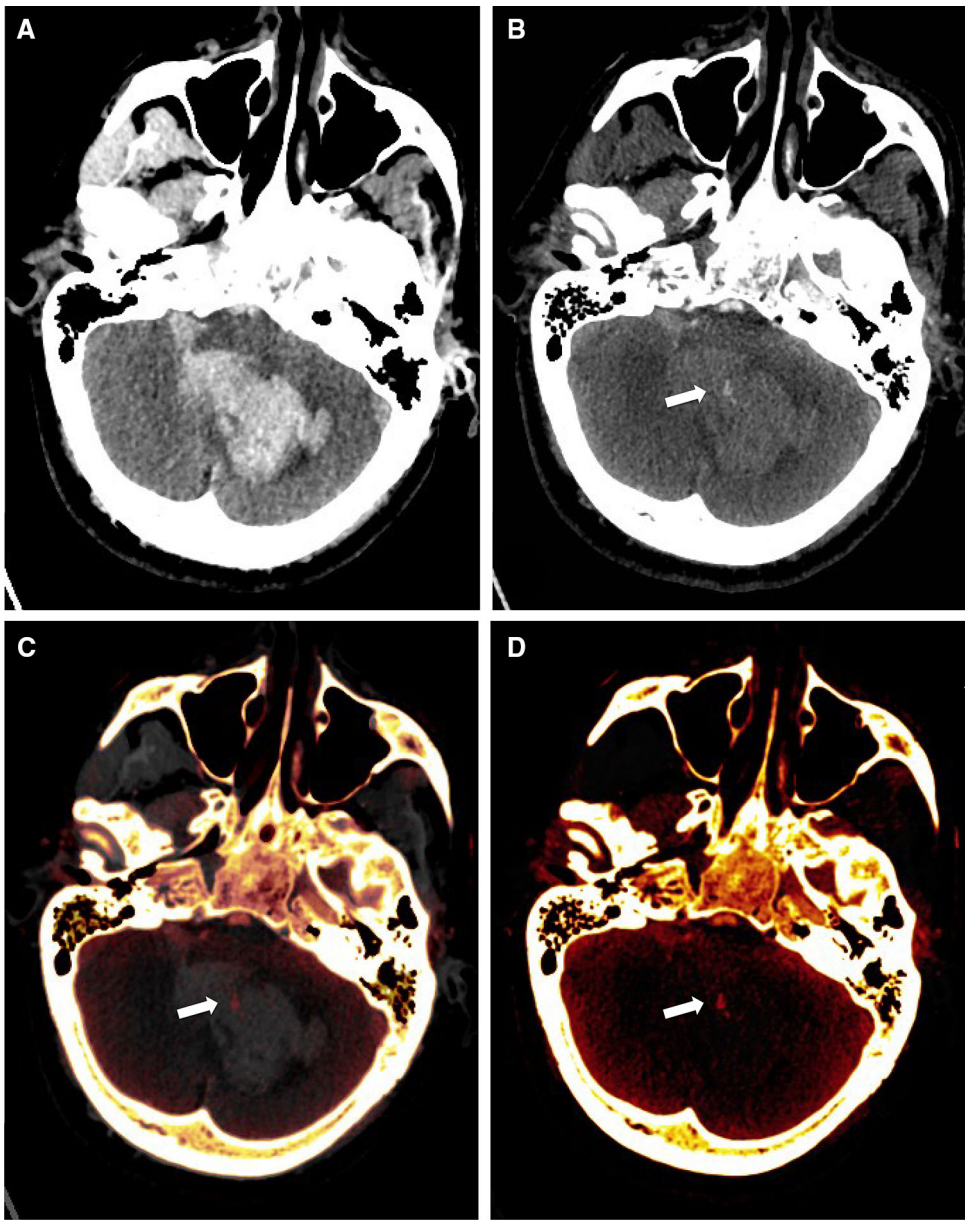

Fig. 2 Spot Sign. **a** Nonenhanced head CT demonstrated left cerebellar intraparenchymal hematoma, **b** CTA demonstrated a focus of higher attenuation (arrow) within the hematoma, corresponding to active bleeding (spot sign). This was confirmed in the dual-energy iodine mapping (**c**, **d**)

It has been shown that the intracranial hemorrhages detected on a per-patient and per-lesion level with DECT are approximately, 100% and 96%, respectively [24].

Cervical Angiography

Another potential use of DECT is for the characterization of carotid atherosclerosis. Despite being a cost-efficient option compared to conventional angiography, DECT for cervical angiography with the application of bone-subtraction techniques enhance the diagnostic accuracy in calculation of the stenotic percentage due to its ability to subtract the calcified plaques. The same principles are applied during lower limb CT angiography. Different bone-subtraction techniques are traditionally applied to avoid this issue in conventional CT arteriography. Both digital subtraction and CT arteriography bone subtraction through unenhanced acquisition have their limitations, including increased radiation exposure and motion artifact between two acquisitions, respectively [25, 26]. Residual bone, vessel truncation, and inadequate vessel delineation are major pitfalls of threshold-based bone subtraction [27]. Compared to unenhanced mask bone subtraction with CT arteriography, DECT bone subtraction provides similar bone removal but better imaging in the cervical region where there is potential for motion. Although unenhanced mask bone subtraction with CT arteriography is ideal for cranial vasculature (due to less motion between image

acquisitions), this comes at the cost of increased radiation doses due to the need to create unenhanced acquisitions [28].

Body

Aortic Imaging

The combination of low kVp images, mixed images, and material removal allows for superior aortic imaging with DECT. Images with dual-source DECT are acquired simultaneously, thus preventing misregistration due to motion, allowing improved subtraction or fusion of images and ultimately better characterization of aortic pathology. It is suggested that DECT should include both mixed images and low kVp imaging [17]. For mixed images, optimal vascular attenuation is achieved with low keV reconstructions. This, however, results in increased image noise [29].

A key strength of DECT in aortic imaging is the use of virtual unenhanced images to reduce radiation dosage. Typically, patients are exposed to a measurable radiation dose when undergoing CT arteriography for acute aortic syndrome, which typically includes nonenhanced and enhanced phases. A nonenhanced phase is often done to determine the presence of intimal calcification or intramural (hyperdense) hematoma in case of an aortic dissection. The yield of the nonenhanced phase is often low, but it is necessary to expose the patient to this radiation to rule out an acute aortic syndrome that may be masked or overlooked on the postcontrast study only. With DECT,

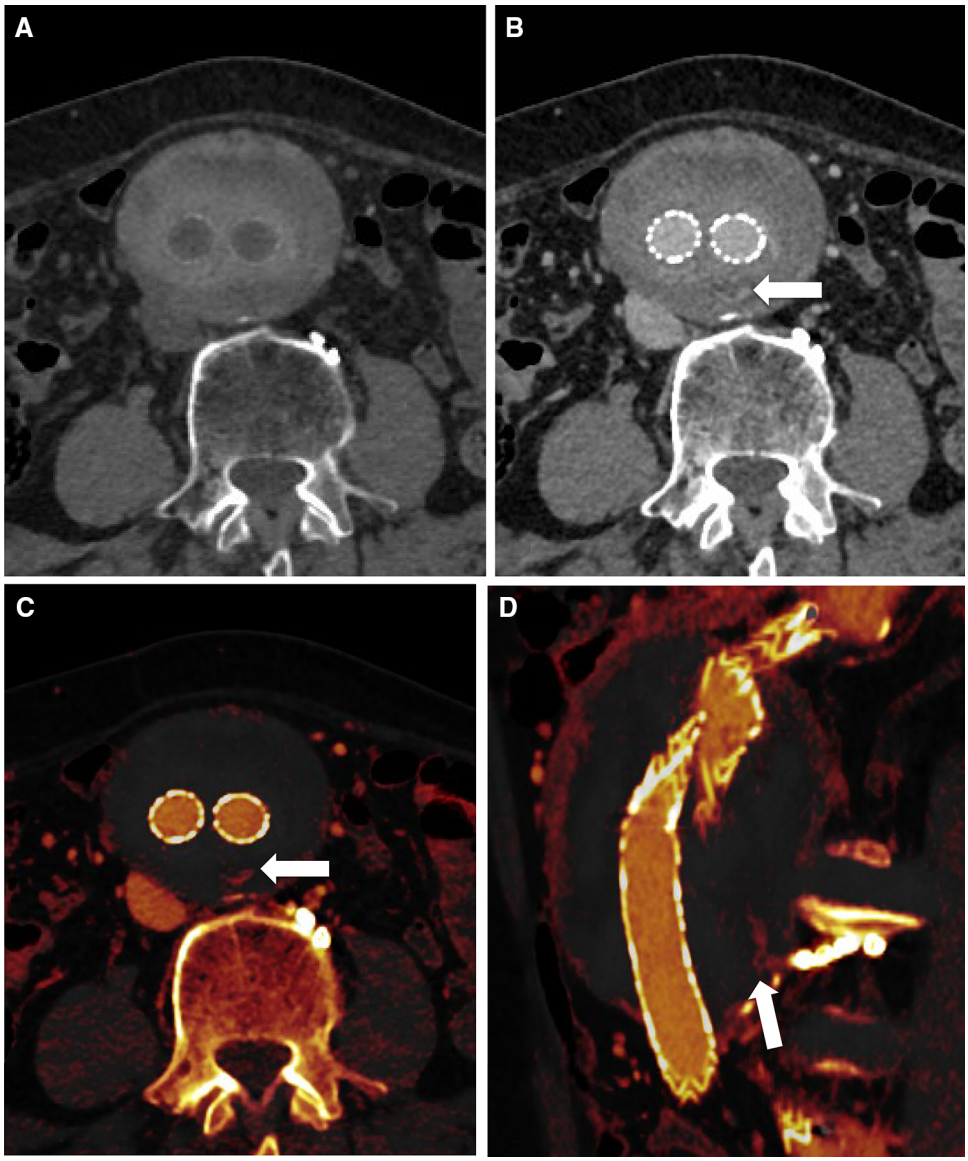

Fig. 3 Type 2 endoleak. **a** Noncontrast CT demonstrated hyper dense areas within the aneurysmal sac (**b**) CTA demonstrated additional subtle linear high attenuation at the posterior aspect of the aneursymal sac "arrow", **c** Iodine map confirmed that this linear high attenuation represents contrast indicating endoleak. **d** CTA, Sagittal reformats showed the endoleak at its relation to the origin of the prior embolized lumbar artery corresponding to type 2 endoleak (arrow)

however, virtual unenhanced imaging is 95% diagnostic and exposes patients to considerably less radiation [30•]. A recent study confirmed that image noise and attenuation measurements were equivalent between both virtual unenhanced imaging and conventional CT imaging [31].

Endoleak Detection

DECT is also extremely useful in detecting endoleaks while minimizing radiation exposure. The typical method of detecting endoleaks in the aorta (after stent repair) involves bi- or tri-phasic imaging techniques (enhanced arterial and delayed imaging) [32]. Patients are often followed lifelong after aneurysm repair, resulting in a substantial cumulative radiation burden. Previous studies support the use of DECT imaging over conventional imaging [33, 34]. In particular, Stolzmann et al. reported DECT with only a single delayed DECT acquisition phase had both a sensitivity and specificity above 96% to detect endoleaks. Accuracy of endoleak detection can be further improved with the iodine selective images produced by DECT (Fig. 3). These images can be grayscale or overlaid on mixed images using a superimposed color. Subtle endoleaks are detected because the overlay maps highlight differences in attenuation due to iodine, blood, or bone [35].

Pulmonary Embolism

One of the key advantages of DECT in chest imaging is for the evaluation of pulmonary embolism. VMIs provide enhanced views of the pulmonary arteries compared to conventional CT. Attenuation to the level of the subsegmental arteries can be achieved with low-energy (< 60 keV) VMIs (Fig. 4). This allows for increased accuracy when assessing pulmonary imaging [36].

Moreover, iodine maps created with the DECT material decomposition technique further help assess perfusion defects caused by pulmonary emboli in a similar way to ventilation–perfusion scans. Iodine maps resemble perfusion images, whereas attenuation of the lung parenchyma with DECT scans resembles ventilation images. Iodine maps can be used to identify areas of pulmonary infarction that appear as nonperfused triangular-shaped areas that are often larger than the pulmonary consolidation revealed when using the lung window view. Conversely, iodine maps in the setting of pulmonary embolism not causing an infarct appear as areas of minor attenuation with no related parenchymal changes. According to Zhang et al., the combination of iodine maps and DECT was found to be 89% sensitive and 92% specific compared to 67% and 100%, respectively, for conventional pulmonary MDCTA [37]. Therefore, iodine mapping is more sensitive at detecting small acute pulmonary emboli (Fig. 5) [37]. With respect to the chronic complications of pulmonary embolism, it is reported that DECT perfusion is more sensitive (100%) and specific (92%) compared to conventional CT at detecting chronic thromboembolic pulmonary hypertension [38•].

Vascular Trauma

In the trauma setting, DECT has an emerging role in identifying sites of active bleeding and detecting

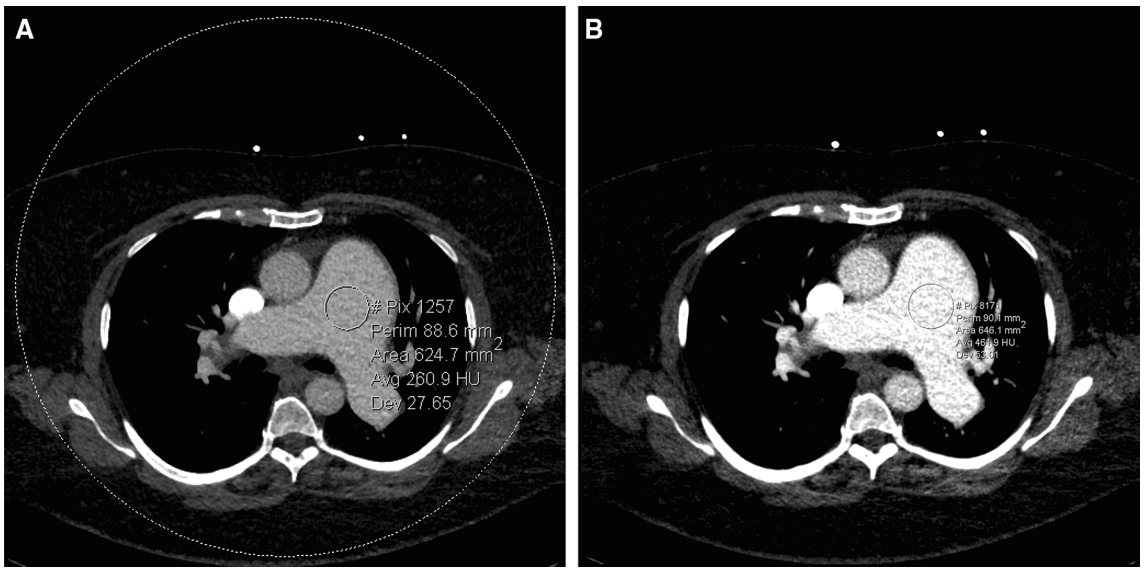

Fig. 4 Contrast optimization. **a** The average attenuation value calculated 260 which is considered suboptimal. **b** After contrast optimization, the average attenuation value increases to 461 HU

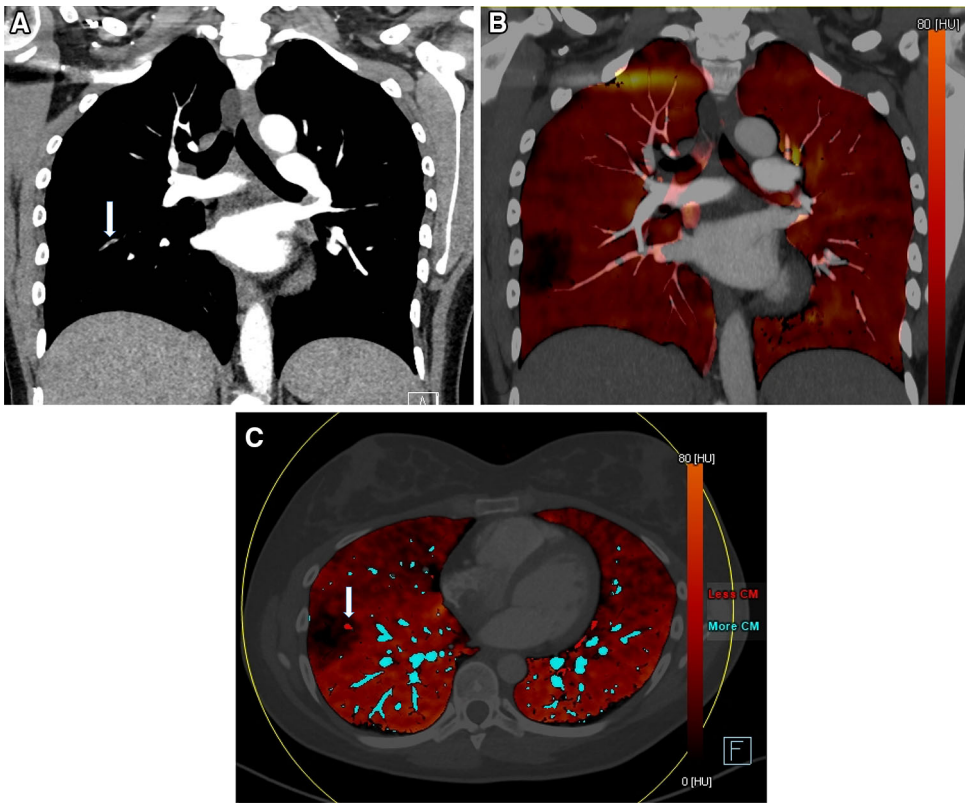

Fig. 5 Iodine mapping (**a**) CTPA coronal slice demonstrated subtle filling defect within a subsegmental branch in the right lower lobe "arrow". **b** Iodine distribution map showed a perfusion defect that corresponds to the filling defect. The emboli is readily visualized in the dual-energy vascular analysis "arrow" (**c**)

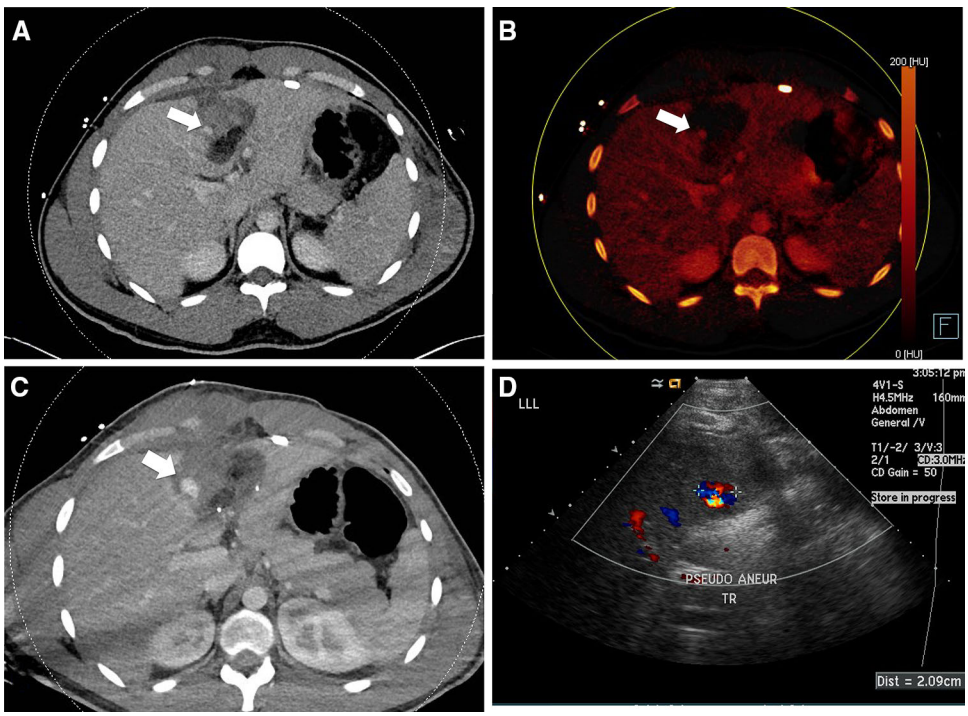

Fig. 6 A 20-year-old male stabbing victim after urgent laparotomy, CT scan shows a complex liver laceration with a subtle rounded high attenuation focus (arrow) in this single portovenous phase (**a**), when correlated with the iodine mapping (**b**), it demonstrates iodine uptake, corresponding to hemorrhagic focus or pseudoaneurysm. Subsequent imaging showing an enlarging pseudoaneurysm "arrow" (**c**) which was confirmed on ultrasound (**d**)

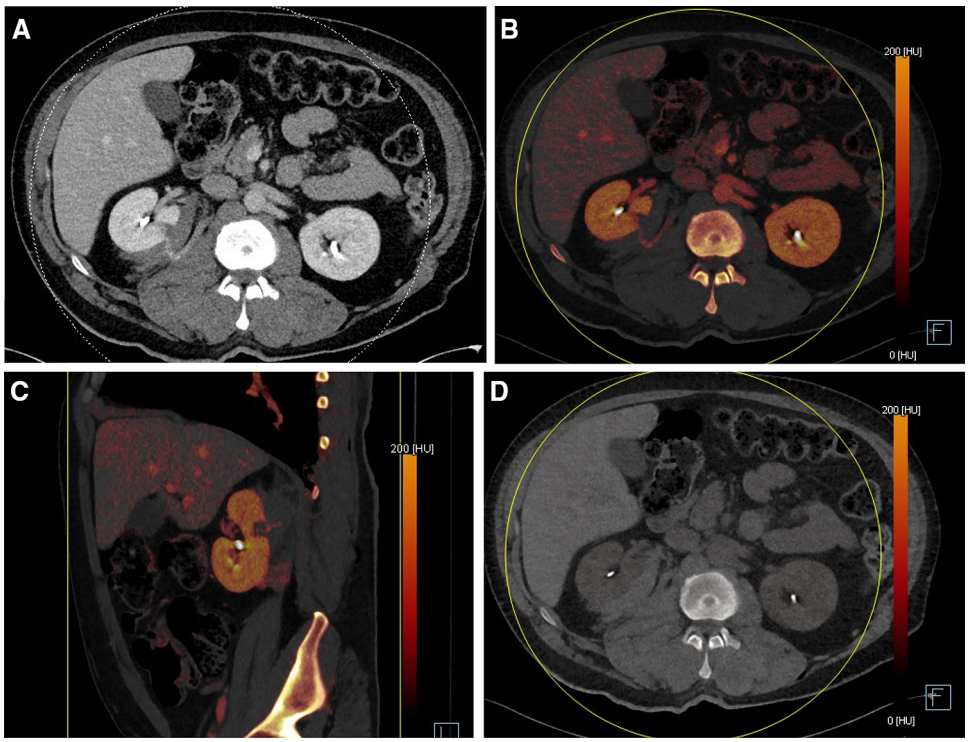

Fig. 7 A 50-year-old male who was stabbed to the right flank. Enhanced CT in portovenous phase (**a**) demonstrated a parenchymal laceration within the posterior right kidney with right perinephric hematoma. Within the hematoma, a linear high attenuation tracking posteriorly, just anterior to the right psoas muscle, suspicious for active bleeding which was confirmed on the dual-energy iodine mapping (**b**, **c**) and was subtracted in the virtual noncontrast image (**d**)

pseudoaneurysms while minimizing radiation exposure. With respect to blunt abdominal trauma, both arterial (~ 30 s after contrast injection) and portal venous (~ 80 s after contrast injection) phases of abdominal CT are acquired. Furthermore, delayed phase imaging (~ 5-10 min after contrast injection) is often required to confirm the presence of active bleeding or a pseudoaneurysm (Fig. 6). Thus, patients undergoing imaging for vascular trauma are exposed to multiple scans resulting in cumulative radiation. Using both virtual unenhanced images and iodine mapping has been found to increase the conspicuity of active extravasation (Fig. 7) while simultaneously reducing radiation exposure [39, 40]. Sun et al. reported that DECT can be utilized to identify active hemorrhage in the bowel and decrease radiation dose by almost one-third compared to standard multiphasic protocols [41••].

DECT is also extremely useful in cases of polytrauma with multiple fractures. For instance, osseous fragments in comminuted pelvic fractures are difficult to differentiate from active extravasation of intravenous contrast with conventional CT as they have similar attenuation. As previously discussed, the material separation processing technique that is unique to DECT allows for small fragments of bone to be subtracted from the image, making it easier for the viewer to identify areas of active intravenous contrast extravasation [42, 43].

Lower Limb Angiography

DECT's high-quality bone-subtraction techniques have a strong advantage over the conventional multidetector CT (MDCT) and digital subtraction angiography employed to investigate vascular pathology in lower limb angiography. Although it is noninvasive with less radiation exposure and scanning time compared to digital subtraction angiography, MDCT comes with the drawback of having a time-consuming Hounsfield unit-threshold-based bone-subtraction technique [44]. DECT is not only more time efficient with respect to bone subtraction in lower limb angiography, but can also create higher-quality images [45, 46]. The bone-subtraction technique employed by MDCT is known to obscure tiny vessels close to bone (such as the dorsalis pedis artery). This can be misinterpreted by the reader as severe stenosis or a complete occlusion of the vessel (Fig. 8). DECT avoids this inherent issue because it relies on the attenuation difference between iodine and calcium [43]. Indeed, sensitivity (97.2%) and specificity (94.1%) for dual-energy bone-subtraction arteriography in the lower limbs are higher than threshold-based bone subtraction (77.1% and 70.7%, respectively) when evaluating clinically significant stenosis (> 75%) [47].

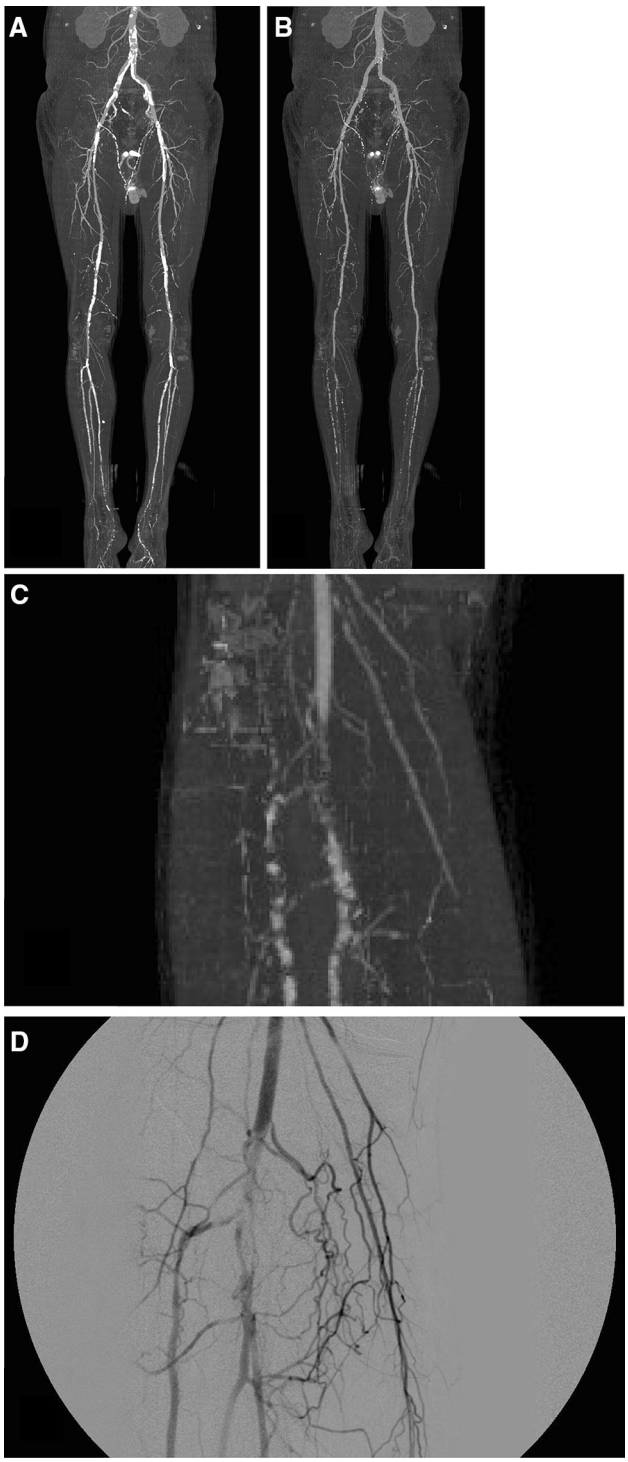

Fig. 8 A 75-year-old male presented with acute right lower limb ischemia. Coronal Thick MIP reformats (**a**) demonstrated extensive atherosclerotic calcification involving the arterial tree of both lower extremities. No definite arterial occlusion is identified. **b**, **c** Utilizing bone-subtraction technique, near occlusion of the distal popliteal artery is readily visualized which was obscured in the conventional CTA due to the blooming artifacts from the dense calcification. This was confirmed in the DSA (**d**)

Conclusions

DECT is a versatile imaging tool that is quickly gaining favor in the field of vascular imaging. Its growing use is mainly based on the unique three-material decomposition techniques and the reconstruction of VMIs. The appropriate use of these techniques often leads to decreased radiation exposure to the patient, reduced interpretation time, and similar (if not superior) diagnostic accuracy compared to the gold standard imaging modalities in the evaluation of vascular pathology such as brain hemorrhage, endoleaks, pulmonary embolism, and vascular trauma.

Disclosures Dr. Khosa is the recipient of the Vancouver Coastal Health – Healthcare Hero Award (2018); the Canadian Association of Radiologists/Canadian Radiological Foundation Leadership Scholarship (2017), and Vancouver Coastal Health Leadership Award (2017).

Compliance with Ethical Guidelines

Conflict of interest Ahmed Alharthy, Matthew D'Mello, Hatim Alabsi, Nicolas Murray, Omar Metwally, Khaled Y. Elbanna, Mohammed F Mohammed, and Faisal Khosa declare no potential conflicts of interest.

Human and Animal Rights and Informed Consent This article contains no studies with human or animal subjects conducted by any of the authors.

References

Recently published papers of particular interest have been highlighted as:
- • Of importance
- •• Of major importance

1. Goldman L. Principles of CT and CT technology. J Nucl Med Technol. 2007;35(3):115–28.
2. Petersilka M, Bruder H, Krauss B, Stierstorfer K, Flohr T. Technical principles of dual source CT. Eur J Radiol. 2008;68(3):362–8.
3. Foley W, Shuman W, Siegel M, Sahani D, Boll D, Bolus D, et al. White paper of the society of computed body tomography and magnetic resonance on dual-energy CT, Part 2. J Comput Assist Tomogr. 2016;40(6):846–50.
4. De Cecco C, Schoepf U, Steinbach L, Boll D, Foley W, Kaza R, et al. White paper of the society of computed body tomography and magnetic resonance on dual-energy CT, Part 3. J Comput Assist Tomogr. 2017;41(1):1–7.
5. De Cecco C, Boll D, Bolus D, Foley W, Kaza R, Morgan D, et al. White paper of the society of computed body tomography and magnetic resonance on dual-energy CT, Part 4. J Comput Assist Tomogr. 2017;41(1):8–14.
6. Siegel M, Kaza R, Bolus D, Boll D, Rofsky N, De Cecco C, et al. White paper of the society of computed body tomography and magnetic resonance on dual-energy CT, Part 1. J Comput Assist Tomogr. 2016;40(6):841–5.

7. Johnson T, Krauß B, Sedlmair M, Grasruck M, Bruder H, Morhard D, et al. Material differentiation by dual energy CT: initial experience. Eur Radiol. 2006;17(6):1510–7.
8. Ali I, Wong W, Liang T, Khosa F, Mian M, Jalal S, et al. Clinical utility of dual-energy CT analysis of bone marrow edema in acute wrist fractures. Am J Roentgenol. 2018;210(4):842–7.
9. Elbanna K, Mohammed M, Huang S, Mak D, Dawe J, Joos E, et al. Correction to: Delayed manifestations of abdominal trauma: follow-up abdominopelvic CT in posttraumatic patients. Abdom Radiol. 2018;43(11):3204–5.
10. Mohammed M, Marais O, Min A, Ferguson D, Jalakhan S, Khosa F et al. Unenhanced dual-energy computed tomography. Invest Radiol. 2017; 1
11. Elbanna K, Mohammed M, Chahal T, Khosa F, Ali I, Berger F, Nicolaou S. Dual-energy CT in differentiating nonperforated gangrenous appendicitis from uncomplicated appendicitis. Am J Roentgenol. 2018;211(4):776–82.
12. Mohammed M, ElBanna K, Ferguson D, Harris A, Khosa F. Pheochromocytomas versus adenoma: role of venous phase CT enhancement. Am J Roentgenol. 2018;210(5):1073–8.
13. Wong W, Shah S, Murray N, Walstra F, Khosa F, Nicolaou S. Advanced musculoskeletal applications of dual-energy computed tomography. Radiol Clin N Am. 2018;56(4):587–600.
14. Lourenco P, Rawski R, Mohammed M, Khosa F, Nicolaou S, McLaughlin P. Dual-energy CT iodine mapping and 40-keV monoenergetic applications in the diagnosis of acute bowel ischemia. Am J Roentgenol. 2018;211(3):564–70.
15. Bonatti M, Lombardo F, Zamboni G, Pernter P, Pozzi Mucelli R, Bonatti G. Dual-energy CT of the brain: comparison between DECT angiography-derived virtual unenhanced images and true unenhanced images in the detection of intracranial haemorrhage. Eur Radiol. 2016;27(7):2690–7.
16. Morhard D, Fink C, Becker C, Reiser M, Nikolaou K. Value of automatic bone subtraction in cranial CT angiography: comparison of bone-subtracted vs. standard CT angiography in 100 patients. Eur Radiol. 2008;18(5):974–82.
17. Vlahos I, Chung R, Nair A, Morgan R. Dual-energy CT: vascular applications. Am J Roentgenol. 2012;199(5_supplement):S87–97.
18. Yuan R, Shuman W, Earls J, Hague C, Mumtaz H, Scott-Moncrieff A, et al. Reduced iodine load at CT pulmonary angiography with dual-energy monochromatic imaging: comparison with standard CT pulmonary angiography—a prospective randomized trial. Radiology. 2012;262(1):290–7.
19. Bamberg F, Dierks A, Nikolaou K, Reiser M, Becker C, Johnson T. Metal artifact reduction by dual energy computed tomography using monoenergetic extrapolation. Eur Radiol. 2011;21(7):1424–9.
20. Mokin M, Kan P, Kass-Hout T, Abla A, Dumont T, Snyder K, et al. Intracerebral hemorrhage secondary to intravenous and endovascular intraarterial revascularization therapies in acute ischemic stroke: an update on risk factors, predictors, and management. Neurosurg Focus. 2012;32(4):E2.
21. Khatri P, Wechsler L, Broderick J. Intracranial hemorrhage associated with revascularization therapies. Stroke. 2007;38(2): 431–40.
22. ••Tijssen M, Hofman P, Stadler A, van Zwam W, de Graaf R, van Oostenbrugge R et al. The role of dual energy CT in differentiating between brain haemorrhage and contrast medium after mechanical revascularisation in acute ischaemic stroke. Eur Radiol. 2013;24(4):834–40. *This study examined 30 active ischemic stroke patients who received intra-arterial treatment. The authors showed that DECT had improved accuracy in discriminating between early contrast extravasation and intracranial hemorrhage.*
23. Wada R, Aviv R, Fox A, Sahlas D, Gladstone D, Tomlinson G, et al. CT angiography "spot sign" predicts hematoma expansion in acute intracerebral hemorrhage. Stroke. 2007;38(4):1257–62.
24. Ferda J, Novák M, Mírka H, Baxa J, Ferdová E, Bednářová A, et al. The assessment of intracranial bleeding with virtual unenhanced imaging by means of dual-energy CT angiography. Eur Radiol. 2009;19(10):2518–22.
25. Tomandl B, Hammen T, Klotz E, Stemper B, Lell M. Bone-subtraction CT angiography for the evaluation of intracranial aneurysms. Am J Neuroradiol. 2006;27(1):55–9.
26. Lell M, Ditt H, Panknin C, Sayre J, Ruehm S, Klotz E, et al. Bone-subtraction CT angiography: evaluation of two different fully automated image-registration procedures for interscan motion compensation. Am J Neuroradiol. 2007;28(7):1362–8.
27. Morhard D, Fink C, Graser A, Reiser M, Becker C, Johnson T. Cervical and cranial computed tomographic angiography with automated bone removal: dual energy computed tomography versus standard computed tomography. Invest Radiol. 2009;44(5):293–7.
28. Lell M, Kramer M, Klotz E, Villablanca P, Ruehm S. Carotid computed tomography angiography with automated bone suppression: a comparative study between dual energy and bone subtraction techniques. Invest Radiol. 2009;44(6):322–8.
29. Behrendt F, Schmidt B, Plumhans C, Keil S, Woodruff S, Ackermann D, et al. Image fusion in dual energy computed tomography: effect on contrast enhancement, signal-to-noise ratio and image quality in computed tomography angiography. Invest Radiol. 2009;44(1):1–6.
30. •Sommer WH, Graser A, Becker CR, Clevert DA, Reiser MF, Nikolaou K, et al. Image quality of virtual noncontrast images derived from dual-energy CT angiography after endovascular aneurysm repair. J Vasc Interv Radiol. 2010; 21(3):315–21. *This study looked at 70 patients after endovascular repair of aortic aneurysms. The authors showed that a single phase DECT protocol (virtual noncontrast images) was reliable in detecting endoleaks with the added benefit of a 44% reduction in radiation compared to a biphasic protocol.*
31. Numburi UD, Schoenhagen P, Flamm SD, Greenberg RK, Primak AN, Saba OI, et al. Feasibility of dual-energy CT in the arterial phase: imaging after endovascular aortic repair. Am J Roentgenol. 2010;195(2):486–93.
32. Stavropoulos SW, Charagundla SR. Imaging techniques for detection and management of endoleaks after endovascular aortic aneurysm repair. Radiology. 2007;243(3):641–55.
33. Chandarana H, Godoy MCB, Vlahos I, Graser A, Babb J, Leidecker C, et al. Abdominal aorta: evaluation with dual-source dual-energy multidetector CT after endovascular repair of aneurysms—initial observations. Radiology. 2008;249(2): 692–700.
34. Stolzmann P, Frauenfelder T, Pfammatter T, Peter N, Scheffel H, Lachat M, et al. Endoleaks after endovascular abdominal aortic aneurysm repair: detection with dual-energy dual-source CT. Radiology. 2008;249(2):692–700.
35. Ascenti G, Mazziotti S, Lamberto S, Bottari A, Caloggero S, Racchiusa S, et al. Dual-energy CT for detection of endoleaks after endovascular abdominal aneurysm repair: usefulness of colored iodine overlay. Am J Roentgenol. 2011;196(6):1408–14.
36. Apfaltrer P, Sudarski S, Schneider D, Nance JW, Haubenreisser H, Fink C, et al. Value of monoenergetic low-kV dual energy CT datasets for improved image quality of CT pulmonary angiography. Eur J Radiol. 2014;83(2):322–8.
37. Zhang L-J, Zhao Y-E, Wu S-Y, Yeh BM, Zhou C-S, Hu X-B, et al. Pulmonary embolism detection with dual-energy CT: experimental study of dual-source CT in rabbits. Radiology. 2009;252(1):61–70.
38. •Dournes G, Verdier D, Montaudon M, Bullier E, Rivière A, Dromer C, et al. Dual-energy CT perfusion and angiography in chronic thromboembolic pulmonary hypertension: diagnostic accuracy and concordance with radionuclide scintigraphy. Eur

Radiol. 2014; 24(1):42–51. *This study examined 40 patients with proven pulmonary hypertension who had both V/Q scintigraphy and DECT perfusion and angiography. The authors demonstrated that DECT perfusion is superior at locating segmental abnormalities.*

39. Uyeda J, Patino M, Sahani D. Dual-energy CT in the acute abdomen. Curr Radiol Rep. 2015;3(6):20.
40. Ali I, Thomas C, Elbanna K, Mohammed M, Berger F, Khosa F. Gastrointestinal imaging: emerging role of dual-energy computed tomography. Curr Radiol Rep. 2017;5(8):31.
41. ••Sun H, Xue H-D, Wang Y-N, Qian J-M, Yu J-C, Zhu F, et al. Dual-source dual-energy computed tomography angiography for active gastrointestinal bleeding: A preliminary study. Clin Radiol. 2013; 68(2):139–47. *This study examined 58 patients with signs of active gastrointestinal bleeding. The authors showed that DECT was both sensitive (88.6%) and specific (100%) for detecting gastrointestinal bleeding, while exposing the patient to only 30% of the radiation dose.*
42. Yeh BM, Shepherd JA, Wang ZJ, Hui ST, Hartman RP, Prevrhal S. Dual-energy and low-kVp CT in the abdomen. Am J Roentgenol. 2009;193(1):47–54.
43. Uyeda J, Anderson SW, Kertesz J, Rhea JT, Soto JA. Pelvic CT angiography: application to blunt trauma using 64MDCT. Abdom Imaging. 2010;17(2):131–7.
44. Willmann JK, Baumert B, Schertler T, Wildermuth S, Pfammatter T, Verdun FR, et al. Aortoiliac and lower extremity arteries assessed with 16-detector row CT angiography: prospective comparison with digital subtraction angiography. Radiology. 2005;236(3):1083–93.
45. Sommer WH, Johnson TR, Becker CR, Arnoldi E, Kramer H, Reiser MF, et al. The value of dual-energy bone removal in maximum intensity projections of lower extremity computed tomography angiography. Invest Radiol. 2009;44(5):285–92.
46. Yamamoto S, McWilliams J, Arellano C, Marfori W, Cheng W, Mcnamara T, et al. Dual-energy CT angiography of pelvic and lower extremity arteries: dual-energy bone subtraction versus manual bone subtraction. Clin Radiol. 2009;64(11):1088–96.
47. Brockmann C, Jochum S, Sadick M, Huck K, Ziegler P, Fink C, et al. Dual-energy CT angiography in peripheral arterial occlusive disease. Cardiovasc Intervent Radiol. 2009;32(4):630–7.